Segmentation of clustered nuclei with shape markers and marking function

Citation: Jierong Cheng, and J.C. Rajapakse. "Segmentation of Clustered Nuclei With Shape Markers and Marking Function." Biomedical Engineering, IEEE Transactions on 56.3 (2009): 741-748. © 2009 IEEE

As Published: http://dx.doi.org/10.1109/TBME.2008.2008635

Publisher: Institute of Electrical and Electronics Engineers

Persistent URL: http://hdl.handle.net/1721.1/52579

Version: Final published version: final published article, as it appeared in a journal, conference proceedings, or other formally published context

Segmentation of Clustered Nuclei With Shape Markers and Marking Function

Jierong Cheng and Jagath C. Rajapakse*, *Senior Member, IEEE*

***Abstract*—We present a method to separate clustered nuclei from fluorescence microscopy cellular images, using shape markers and marking function in a watershed-like algorithm. Shape markers are extracted using an adaptive H-minima transform. A marking function based on the outer distance transform is introduced to accurately separate clustered nuclei. With synthetic images, we quantitatively demonstrate the performance of our method and provide comparisons with existing approaches. On mouse neuronal and Drosophila cellular images, we achieved 6%–7% improvement of segmentation accuracies over earlier methods.**

***Index Terms*—Active contours, cell segmentation, cellular imaging, fluorescence microscopy, watershed segmentation.**

I. Introduction

VISUAL inspection of cellular images is often insufficient to detect or describe subtle but important changes in cellular morphology. To adequately characterize subtle features and changes in tissues, a quantitative assessment of cellular morphology is often desired. The primary step in quantitative analysis of cell shape and motion is usually the identification or segmentation of individual cells or cell nuclei. Currently, this is mostly performed manually or using semiautomatic tools available in microscopic image analysis software. However, manual segmentation of nuclei in microscopic images could be very labor-intensive and even infeasible.

Segmentation tools commonly distributed with microscopy software (for example, MetaMorph Imaging Software by Molecular Devices) are usually based on classical techniques such as correlation matching, thresholding, or morphological operations. These methods suffer considerably due to overgeneralization, limiting their use on images gathered in cell biology research. Correlation matching, for instance, fails for cells that change shape in noisy environment and generally requires users manually define the position of every cell in the first frame. Segmentation methods based on global thresholding fail for images that exhibit strong intensity gradients and/or noise. Preprocessing with smoothing filters and adaptive thresholding helps but could lead to merging touching cells or nuclei. Watershed transforms prevent such merging but usually lead to oversegmentation unless markers are manually chosen. To overcome such limitations, existing software tools often allow the users to interactively correct trajectories or segmentation through user-friendly interfaces. As a result, however, the benefits of automation such as speed, reproducibility, and objectivity tend to be lost. User interaction is a bottleneck for high-throughput imaging applications. Therefore, the development of more reliable and automated image analysis techniques for cellular imaging remains an important goal in computational molecular biology.

In recent years, many image analysis approaches have been adopted for cell and nuclei segmentation from microscopic images. Active contours compute segmentations of a given image by evolving contours in the direction of the negative gradient of image energy. Traditional edge-based active contour methods [1], [2], where the image energy is computed by the integral of a locally computed edge map along the contour, render poor results on fluorescence microscopy images especially when the boundaries are fuzzy and sensitive to initialization. Various new models of active contours have emerged to improve evolution of curves [3]. On the other hand, geometric active contours based on level sets are becoming increasingly popular because they neither require any explicit parameterization nor suffer from any constraints on the topology as snakes. In the model of active contours without edges [4], the image energy terms are computed using intensity variances inside and outside the contour. This region-based approach provides strong robustness to noise and allows segmentation of cells with blurred edges. The approach has been used for segmenting and tracking cells in 2-D images [5] and dynamics of 3-D images [6].

Other promising methods for cell or nuclei segmentation include watershed algorithm [7], [8], multiscale analysis [9], dynamic programming-based methods [10], [11], graph-cut methods [12], and Markov random fields [13]. By analyzing the edges at different spatial scales, multiscale techniques can handle images with weak edges and nonuniform intensity variations but they are unable to handle the edges of overlapping nuclei with minimal or no edge information [9]. Recently, a semiautomatic method for detection of optimal boundaries was proposed [10], [11], which is defined as the path having the highest average intensity along its length compared to all other possible paths and obtained using dynamic programming. Graph-cut-based methods optimize segmentation energies by combining a wide range of visual cues and constraints, and are related to active contour methods [12]. However, optimal boundary and

Manuscript received January 29, 2008; revised July 15, 2008 and September 22, 2008. First published November 11, 2008; current version published April 15, 2009. This work was supported in part by the Computation and Systems Biology Programme of Singapore–Massachusetts Institute of Technology (MIT) Alliance. *Asterisk indicates corresponding author*.

J. Cheng is with the School of Computer Engineering, Nanyang Technological University, Singapore 638798, Singapore, and also with the Computation and Systems Biology Programme, Singapore–Massachusetts Institute of Technology (MIT) Alliance, Nanyang Technological University, Singapore 637460, Singapore (e-mail: jrcheng@ntu.edu.sg).

*J. C. Rajapakse is with the School of Computer Engineering, Nanyang Technological University, Singapore 638798, Singapore, and also with the Department of Biological Engineering, Massachusetts Institute of Technology (MIT), Cambridge, MA 02139 USA (e-mail: asjagath@ntu.edu.sg).

Color versions of one or more of the figures in this paper are available online at http://ieeexplore.ieee.org.

Digital Object Identifier 10.1109/TBME.2008.2008635

graph-cut methods depend on manual marking of each cell for algorithm initiation. A nuclear segmentation algorithm based on Gaussian Markov random fields suffers from undersegmentation and high false positives [13].

One main challenge in nuclei or cell segmentation is the separation of touching objects. The gradient flow tracking method finds the corresponding center that each point floods to find the boundaries between touching cells [14]. The method may have difficulty in processing images composed of textured blob cells. The classical watershed algorithm directly uses region minima or ultimate eroded points (UEPs) as seed points [15]. Although it can delineate touching objects, oversegmentation is likely to happen at the same time. There are two proposals to handle this problem: region merging and marker-controlled watershed. Region merging approaches could be based on shape or sizes of cells or nuclei [8], [16], [17].

A marker-controlled watershed algorithm replaces region minima or UEP with predefined markers, each representing an object [18]. Although marker-based methods effectively handle oversegmentation problem, it only works on the premise that the extracted markers really represent the true objects. Thus, the difficulty in adopting this method is the accurate extraction of markers. The proposed method in [19] successfully extracts cell makers, and thereby segments cells but is limited for objects with descending intensity and having round shape. A marker extraction method based on condition erosion was proposed in [20] but the results were sensitive to the sizes of erosion structures and the thresholds of condition erosions. The marker detection algorithm in [21] combines the photometric and shape information in a framework of pattern classification that decides whether markers should be merged. However, the marking function used for watershed flooding was not mentioned and no graphic segmentation results are given to indicate the accuracy of watershed lines.

Our aim is to develop a fully automatic method for segmentation of nuclei in tissues from 2-D microscopy images. We specially address the issue of segmentation of nuclei that overlap or touch each other, or in the phase of cell division. The initial segmentation is based on active contours. In order to detect and separate clustered nuclei in a more robust and precise way, in this paper, we present a method to find shape markers and a new marking function to use in a watershed-like segmentation. The manuscript is organized as follows. Section II describes the proposed method in detail. In Section III, we show experiments on synthetic data as well as on two microscopic images obtained from mouse neurons and Drosophila cells. With synthetic data, we quantitatively demonstrate our method and provide comparisons to earlier methods. With real data, we achieved 6%–7% improvement of segmentation accuracy over earlier methods. In Section IV, conclusions and future work are presented.

II. Method

The method begins with an initial segmentation of nuclei, using active contours without edges. Then, a marker-controlled watershed algorithm with a new marking function capable of accurately separating clustered nuclei is applied.

A. Object Segmentation

For the segmentation of nuclei from background, the model of active contours without edges was adopted [4]. In traditional edge-based active contours, image energy is taken as the integral of locally computed features along the contour. In contrast, region-based methods compute image energy from surface integrals over the entire image. More specifically, image energy is defined using intensity variances inside and outside of the contour. Therefore, region-based models are robust to noise and allow segmentation of objects with blurred edges. The active contours are implicitly represented by a single level set function and changes in objects appear automatically as the level set function evolves. This enables automatic detection of an arbitrary number of objects from an arbitrary initial front. We chose to initialize the level set function as a small circle at the center of the image.

The energy function of the active contour is based on a reduced form of the Mumford–Shah function for image segmentation

$$\begin{aligned} E(\phi, \mu_I, \mu_O) = \alpha \int_x \int_y \delta(\phi)|\nabla\phi| \mathrm{d}x\, \mathrm{d}y \\ + \lambda_I \int_x \int_y \mathcal{H}(\phi)(g-\mu_I)^2 \mathrm{d}x\, \mathrm{d}y \\ + \lambda_O \int_x \int_y (1-\mathcal{H}(\phi))(g-\mu_O)^2 \mathrm{d}x\, \mathrm{d}y \end{aligned} \quad (1)$$

where $\Omega \subset \mathbf{R}^2$ is the 2-D domain of image g and $(x, y) \in \Omega$. ϕ is a level set function defined on Ω, whose zero-level set $\{(x, y) \in \Omega | \phi(x, y) = 0\}$ defines the segmentation such that $\phi > 0$ inside the segmented objects and $\phi < 0$ outside. μ_I and μ_O are, respectively, the mean intensity of pixels inside and outside the zero level set. $\mathcal{H}$ and δ are the Heaviside and Dirac functions. λ_I, λ_O, and α are fixed positive parameters.

The minimization of image energy is accomplished by letting the level set function evolve as a function of an abstract time t, starting from an initialization $\phi(t = 0, x, y)$ according to

$$\frac{\partial \phi}{\partial t} = \left(\alpha \nabla \frac{\nabla \phi}{|\nabla \phi|} - \lambda_I (g-\mu_I)^2 + \lambda_O (g-\mu_O)^2 \right) \delta(\phi). \quad (2)$$

Here $\nabla(\nabla\phi/|\nabla\phi|)$ is the (mean) curvature of the level set, generating a regulating force that smoothens the contours. The other two forces on the right-hand side move the contour toward the actual boundary of objects.

After nuclei are segmented by active contours, the segmentation was refined by a series of morphological operations. First, the holes within segmented nuclei are filled as they could affect the result of subsequent distance transforms and cause incorrect separation of clusters. Thereafter, tiny objects unlikely to be the fragments of real nuclei are discarded by performing morphological opening with a disc structuring element.

B. Shape Markers

The watershed segmentation algorithm uses a relief function f, usually the gradient of the intensity, giving the altitudes

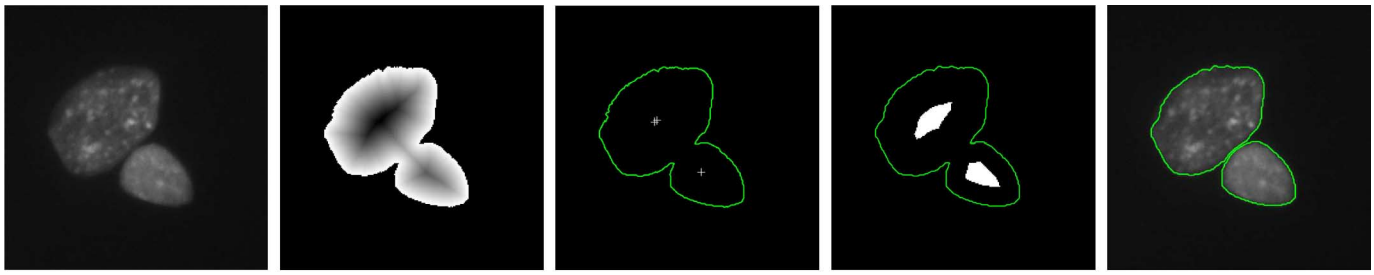

Fig. 1. Markers and separation of nuclei by a marker-controlled watershed algorithm. (a) Original image. (b) Inner distance map generated after initial segmentation. (c) Regional minima of (b). (d) Shape markers obtained from adaptive H-minima transform with $\Delta = 2$. (e) Results of segmentation.

of a topographic surface from its regional minima. The watershed line is generally a set of points equidistant to the regional minima of the relief function measured by a topographic distance and often used in segmentation objects in images [15]. Marker-controlled watersheds flood from the markers that can be regarded as the first estimation of the image partitioning [18].

We use the initial segmentation of nuclei obtained by active contours to generate markers by using an *inner distance transform*. The inner distance transform converts the binary image, consisting of foreground and background pixels, into a distance map measured using Euclidean distance, where every foreground pixel has a value corresponding to the minimum distance from the background. The regional minima of the inverse of the inner distance map are regarded as markers.

H-minima transform is often used to prevent oversegmentation. It suppresses all minima, less than a particular depth h of the relief function [22]. In other words, the intensity of the transformed image is controlled by a minima suppression parameter h, lower values of which could lead to oversegmentation while higher values may fail to separate touching objects. In this way, H-minima transform suppresses undesired minima.

We presume that there exists one-to-one correspondence between the markers and the objects. To accurately find the value of h, an *adaptive H-minima transform* is introduced to extract the correct number of markers and minimize any over- and undersegmentation of nuclei. In the adaptive H-minima transform, the depth threshold is increased until before a merger of the regions begins. Let H-minima transform on inverse inner distance map g_I of the image at threshold h be $H(g_I, h)$, S be the set of all connected regions resulted from initial segmentation, and $N^j(h)$ be the number of minima within connected region $j \in S$ after applying the transform. The adaptive H-minima transform algorithm learns h adaptively as h_{adp} as follows:

begin: Adaptive H-minima Transform
$h_{\mathrm{adp}} = 1$;
Find $H(g_I, h_{\mathrm{adp}})$
for connected region $j \in S$ **do**
  $h = h_{\mathrm{adp}}$;
  if $N^j(h_{\mathrm{adp}}) > 1$ **then**
    repeat
      $h = h + 1$;
      Find $H(g_I, h)$
    until $N^j(h) < N^j(h_{\mathrm{adp}})$
    $h_{\mathrm{adp}} = h - \Delta$;
  else
    $h_{\mathrm{adp}} = h$;
  end if
  Find $H(g_I, h_{\mathrm{adp}})$
end for

The regional minima obtained after $H(g_I, h_{\mathrm{adp}})$ correspond to the *shape markers* for objects. The shape markers demonstrate not only the number and location but also characterize the shape of nuclei, and help in generating the marking function. The adaptive H-minima transform finds the depth threshold before minima start to merge or disappear. By properly selecting gap parameter Δ, undesired regional minima are removed, and thus the number of nuclei contained in each object is accurately determined. The value of Δ depends on the profile of the distance function, and therefore on the shapes and size of the clusters. The resulted shape markers provide information of the number, location, and shape of nuclei, and are used as the set of minima to impose onto the marking function. The adaptive H-minima transform is illustrated on two representative clustered nuclei in Fig. 1.

C. Marking Function

The segmentation by watershed algorithm depends not only on the markers but also on the marking function f—the topographic surface flooded by water. A good marking function should synthesize physical characteristics of the objects to segment and have different markers and catchment basins characterizing the desired objects.

For separation of partially overlapping objects in binary images, the inverse inner distance map is chosen as the classical marking function [15]. The inner distance transform generates a valley connecting the minima [see Fig. 2(a)]. In the hill climbing implementation of watershed [23], an approximation is necessary to provide an ordered queue to pixels of the same gray level. This secondary ordering is based on the order in which pixels are reached by a flooding region, assuming that the distances between the center and its neighbors in four or eight connected neighborhoods are equal. That is, there is no penalty for a diagonally connected pixel. This approximation of the marking function often results in jagged watershed lines [24], as it uses a chessboard distance pattern in place of Euclidean distance to compute the distance function across plateaus. Unlike Euclidean

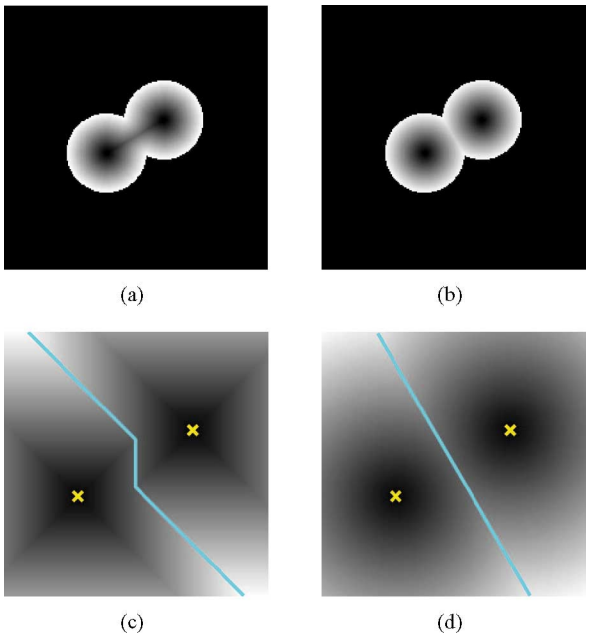

Fig. 2. Euclidean distance map using (a) inner distance transform and (b) outer distance transform. The distance map of two pixels, created by (c) the chessboard distance and (d) the Euclidean distance.

distance whose equidistant line from two points is a straight line [see Fig. 2(d)], the equidistant line of chessboard distance consists of three vertical/horizontal or diagonal segments as its propagation take a squarely shape [see Fig. 2(c)].

We propose a new marking function based on outer distance transform to avoid jagged boundaries of segmented objects. The *outer distance transform* converts a binary image into a distance map where every background pixel has a value corresponding to the minimum distance from shape markers. As the outer distance transform measures the distance from the shape markers, resulting distance map resembles the shape of nuclei. The outer distance transform generates a single pixel width ridge line [see Fig. 2(b)] that watershed finds correctly irrespective of the implementation algorithm used and results in a straight watershed line.

Given an initial segmentation and shape markers $\mathcal{M} = (\mathcal{M}_1, \mathcal{M}_2, \ldots, \mathcal{M}_K)$, the new marking function is generated as follows.

1) Calculate the Euclidean distance transform

$$D_i(x) = \inf_{y \in \mathcal{M}_i} D(x, y) \tag{3}$$

where $D(x, y)$ is the Euclidean distance between points x and y, and $D_i(x)$ corresponds to the minimum distance between x and the shape marker $\mathcal{M}_i$.

2) Obtain the marking function by

$$f(x) = \min_i \{d_i + D_i(x)\} \tag{4}$$

where d_i is the level (value) of the marking function f on $\mathcal{M}_i$. Since we consider f as a 3-D topographic surface, the function value corresponds to the level/height of the surface.

The Euclidean outer distance map generates the marking function from the markers, representing shape characteristics of the object. The difference between the new marking function (4) based on outer distance and the classical relief function used in the watershed algorithm is that the topographical distance is replaced with the geodesic distance. For connected convex shapes, the geodesic distance is equivalent to Euclidean distance. If the relief function f is itself a distance function (i.e., $|\nabla f| = 1$), the topographical distance reduces to the geodesic distance and the watershed becomes identical with the geodesic skeleton by zone influence [25]. In addition, the levels of different markers are accounted for (4). The watershed lines are generated thereafter based on a simulated flooding process on the Euclidean outer distance map.

III. Experiments and Results

We demonstrate the efficacy of our method on synthetic images as well as on real microscopic images of mouse neurons and Drosophila cells. We compare the segmentation by the present method with earlier techniques such as classical watershed, condition erosion, and optimal boundary finding by dynamic programming.

A. Synthetic Images

Two binary circular nuclei partially clustered with each other were synthetically created. The segmentation accuracy by the present method was tested with increasing Gaussian noise. The effects of watershed segmentation using two different marking functions are illustrated in Fig. 3. In contrast to the jaggedness generated by the classical marking function based on the inner distance [see Fig. 3(c)], the proposed outer distance marking function using shape markers generated straight boundaries separating the nuclei as desired [see Fig. 3(e)].

The accuracy of separation by the proposed marking function is tested on a set of synthetic images obtained by changing the orientation θ of the line connecting centroid with respect to the horizontal line, as shown in Fig. 4. The accuracy of watershed lines obtained using the classical marking function, geometric analysis, and the present method are given in Fig. 5. The ground truth of the boundary of two objects is given by a straight line normal to the line connecting the centroids. The classical watershed creates jagged edges and the errors become minimum when $\theta = 0^\circ, 45^\circ, 90^\circ, 135^\circ$, etc. The error is measured by the area of triangles marked by the gray zone in Fig. 5. Using the conventional method of half base times height, the error is given by

$$error(\theta) = \begin{cases} \dfrac{1}{\sqrt{2}} a^2 \sin(\theta) \sin(45^\circ - \theta), \text{when } 0^\circ \le \theta \le 45^\circ \\ \dfrac{1}{\sqrt{2}} a^2 \cos(\theta) \sin(\theta - 45^\circ), \text{when } 45^\circ < \theta \le 90^\circ \end{cases} \tag{5}$$

where a is the half of the length of ground truth line. We measure the accuracy as area correlation, i.e., the intersection/union of the areas enclosed by the estimated boundary and the desired boundary. The watershed segmentations obtained using different

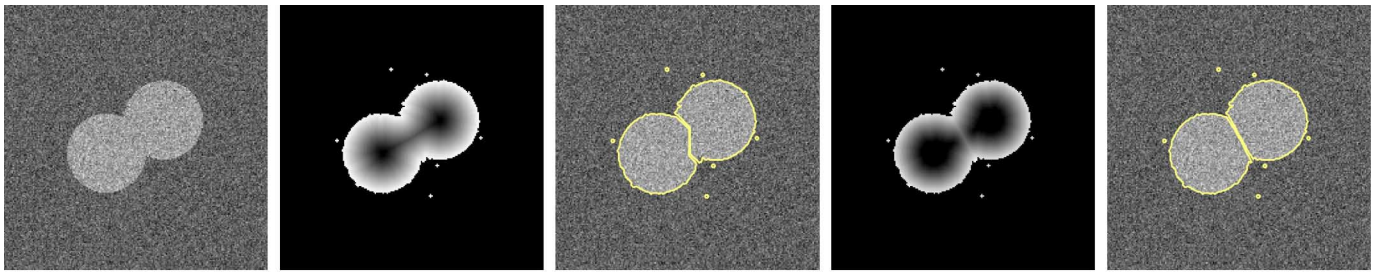

Fig. 3. Separation of nuclei. (a) Original synthetic image with Gaussian white noise (SNR = 8 dB). (b) Inner distance map. (c) Watershed segmentation using inner distance map as marking function. (d) Outer distance map generated with shape markers and $\Delta = 2$. (e) Final segmentation using the outer distance map as the marking function.

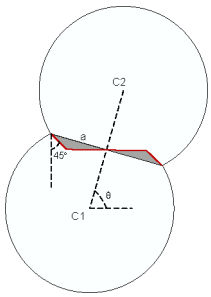

Fig. 4. Shaded triangles show the errors due to jagged lines created by classical watershed algorithm using inner distance map as the marking function.

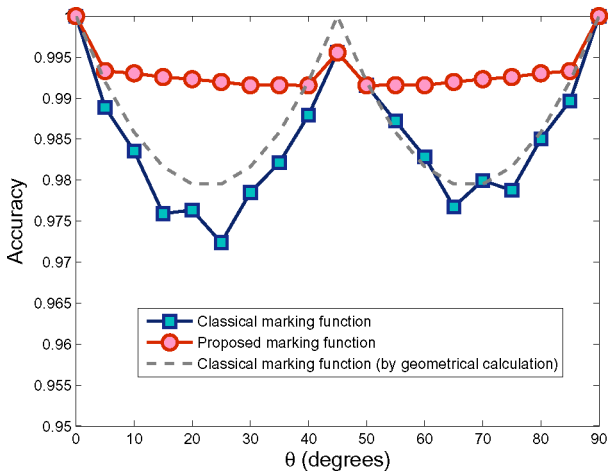

Fig. 5. Accuracy of segmentation of synthetic images, using different marking functions against tilt angle.

marking functions are compared with the ground truth segmentation, and the area correlation measured for different values of θ is shown in Fig. 5. The difference between the experimental results and geometrical calculation is due to the discretization and the added noise.

The performances of the proposed marking function and the classical marking function on synthetic images with the presence of noise are given in Fig. 6. As seen, the proposed marking function segments the clusters more precisely than the classical marking function at all noise levels. The method fails only when the SNR drops below about 4 dB.

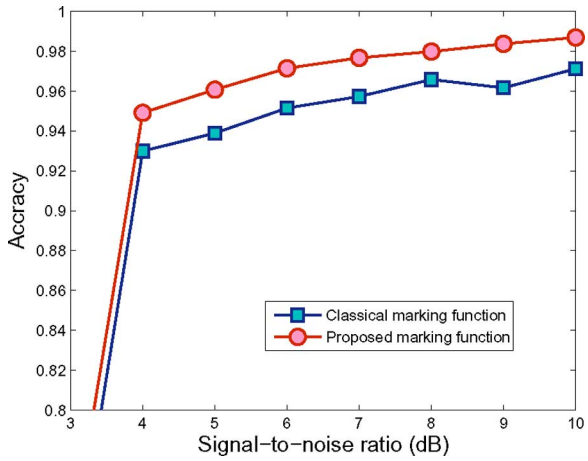

Fig. 6. Robustness of object separation to noise on synthetic images.

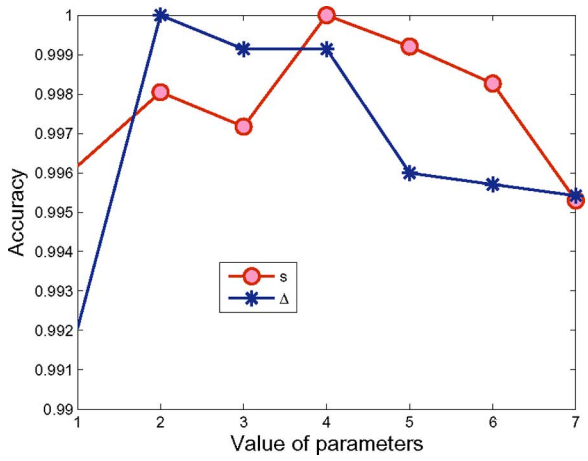

Fig. 7. Sensitivity of parameters on the performance of cluster separation: the diameter of the structuring element s and tolerance value of the adaptive threshold Δ (in pixel values).

B. Sensitivity to Parameters

The parameters of the active contours were empirically set to $\alpha = 0$, $\lambda_I = 1.5$, and $\lambda_O = 1.0$. μ_I and μ_O were computed iteratively in the algorithm. There are two parameters that affect the separation of clusters. One is the kernel size s of the

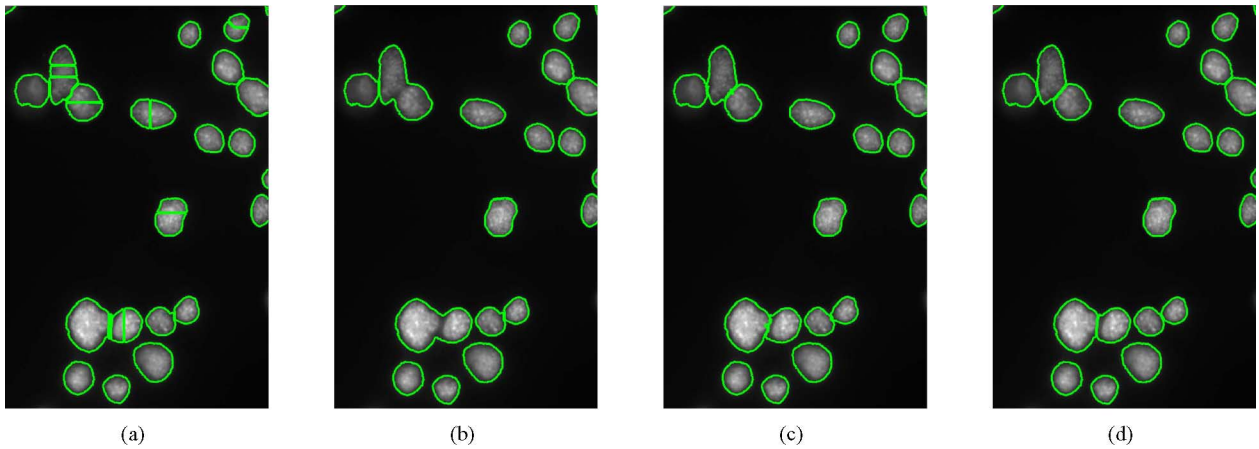

Fig. 8. Results of nuclei segmentation on a representative neuronal cell image by. (a) Classical watershed. (b) Condition erosion watershed. (c) Optimal boundary by dynamic programming. (d) Proposed algorithm ($\Delta = 5$).

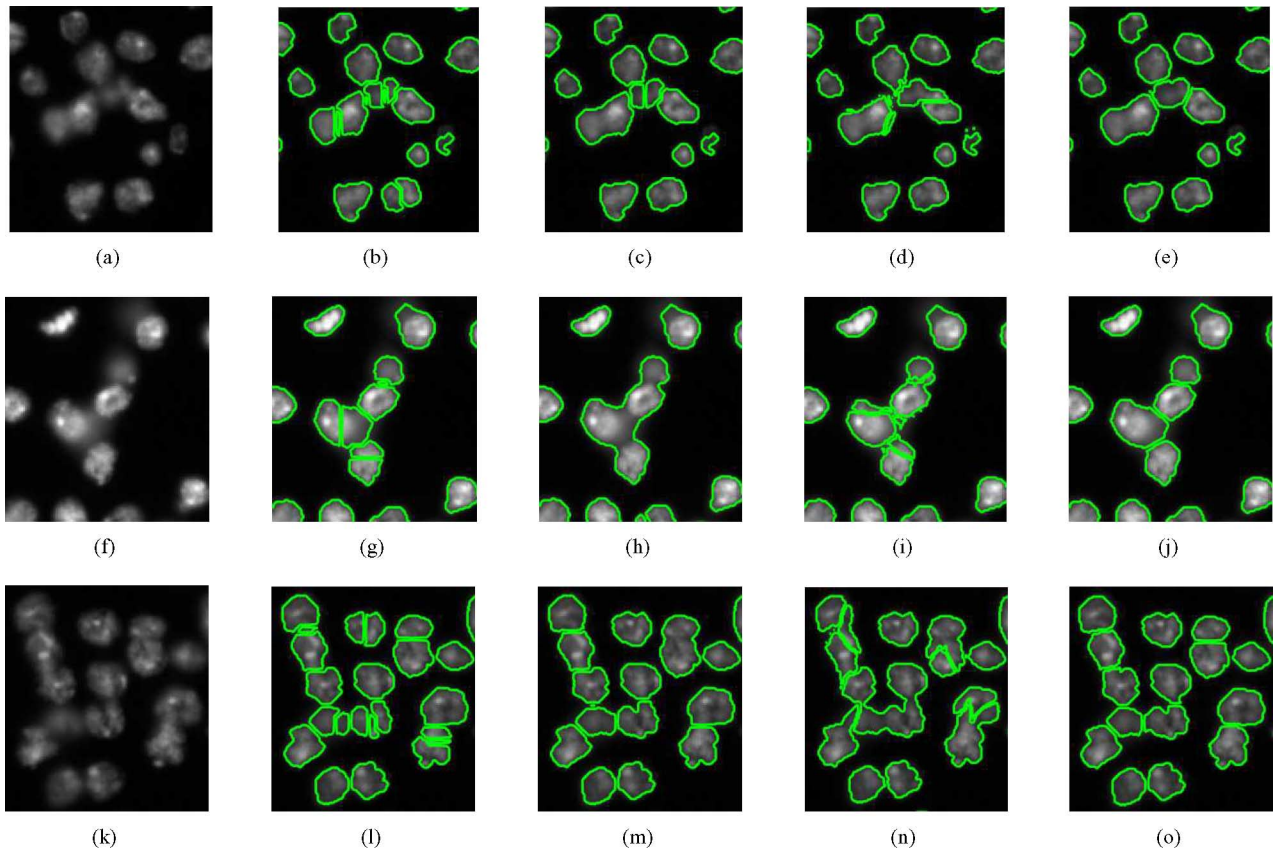

Fig. 9. Nuclei segmentation on three Drosophila cell images. (a) Original images. (b) Classical watershed. (c) Condition erosion watershed. (d) Optimal boundary by dynamic programming. (e) Proposed algorithm ($\Delta = 5$).

structural element used in the opening during initial segmentation. Smoother object boundaries are obtained when s is increased at the expense of accuracy. The other is Δ in the adaptive H-minima transform, which determines the gap between shape markers. Note that adaptive H-minima transform is performed on each cluster, and each cluster has its own largest H-minima transform (h_{adp}). So, the resulting h_{adp} is adaptive to each cluster. The value of Δ was empirically found in the experiments and in the range $[2,\ 5]$. If properly selected small enough, the same value of Δ can be used throughout the image.

For images in Fig. 1(a), $s = 4$ and $\Delta = 2$ were found to give the best separation (units are in pixels). By considering the separation result displayed in Fig. 1(e) as the ground truth, we test the robustness of our algorithm by varying the values of the parameters; the accuracies against parameter values are given in Fig. 7. As seen, the errors were less than 0.5% for changes within $[2, 7]$ pixel values of the parameters.

TABLE I
COMPARISON OF SEGMENTATION BY THE PROPOSED METHOD AND EXISTING METHODS ON IMAGES OF NEURONAL CELL NUCLEI

Method	Correctly segmented	Over-segmented	Under-segmented	Correctly segmented from clusters
Classical watershed	66.58 %	33.42 %	0.00%	67.61 %
Condition erosion	90.34 %	3.92 %	5.74 %	66.20 %
Proposed method	97.39 %	1.83 %	0.78 %	95.77 %

TABLE II
COMPARISON OF SEGMENTATION BY THE PROPOSED METHOD AND EXISTING METHODS ON IMAGES OF DROSOPHILA CELL NUCLEI

Method	Correctly segmented	Over-segmented	Under-segmented	Correctly segmented from clusters
Classical watershed	81.48 %	18.52 %	0.00%	66.67 %
Condition erosion	88.89 %	1.62 %	9.50 %	50.08 %
Proposed method	96.30 %	3.24 %	0.46 %	86.46 %

C. Real Images

We performed segmentation of nuclei on two real datasets: neuronal cell images and Drosophila cell images. The neuronal cells of mouse brain contained 53 fluorescence microscopy images of 1392×1040 pixels. The imaging was performed on a Zeiss Axio Imager Z1 equipped with a Plan-Apochromat $20\times/0.75$ objective. The images were recorded with a programmable virtual camera (PVCAM) and tagged to extract the nuclei. There were a total of 383 nuclei out of which 71 were clustered. The dataset of Drosophila Kc167 cells contained four microscopy images of 450×450 pixels. There were 432 nuclei in total, out of which 96 were clustered. The details of Drosophila images are available in [26].

To demonstrate the efficacy of cluster identification, we compared our method to the classical watershed algorithm [15], marker-controlled watershed using condition erosion [20], and optimal boundary finding by dynamic programming as proposed by Baggett *et al.* [10]. The classical watershed algorithm uses region minima of inner distance map as markers while the condition erosion algorithm detects markers with a "first coarse, then fine" erosion strategy. Both of the two methods adopt Euclidean inner distance map as the marking function. In optimal boundary finding by dynamic programming, the user is required to indicate a point approximately in the center of the cell and a point on the border that encompasses two or more cells. In our implementation, the border points were automatically approximated by the point at the middle of the centers of clustered nuclei. Since the border between the clustered nuclei is of relatively lower intensity than surrounding pixels, the optimal path is defined as the path that has the lowest average intensity along its length compared with all other possible paths.

Examples of nuclei segmentation results are displayed in Figs. 8 and 9. The classical watershed algorithm suffered from oversegmentation, and the condition erosion algorithm occasionally undersegmented or oversegmented the clusters because of incorrect detection of markers. In contrast, the proposed method generated more precise segmentation while removing the jaggedness of boundaries. The boundary generated by the dynamic programming method tends to be irregular and even incorrect when the number of nuclei in a cluster increases or the intensity contrast along the border is low. The performance of this method is found to be highly dependent on user input and intensity contrast. Compared to the dynamic programming method, the proposed method separated the clusters using shape information and is found to be more robust to intensity variations of nuclei.

The comparison of segmentation results with different methods is shown in Tables I and II. From neuronal cell images and Drosophila cell images, 97.39% and 96.30% of cell nuclei were correctly segmented, respectively. As seen, the classical watershed algorithm had produced high oversegmentations whereas the difficulty of the condition erosion method lies in the setting of erosion structure size and it cannot ensure the existence of proper thresholds to prevent both oversegmentation and undersegmentation. The proposed method outperformed the other methods and was able to segment most touching nuclei correctly from clusters.

IV. CONCLUSION

We presented an automated technique to segment cell nuclei in fluorescence microscopy images, which is capable of accurately separating clustered nuclei. The method relies on geometric active contours for initial segmentation, and thereafter on a watershed-like algorithm using shape markers and marking function. An adaptive H-minima transform was proposed to accurately find shape markers, avoiding oversegmentation. The shape markers convey not only the number and location of nuclei but also represent shapes of the nuclei. A new marking function based on outer distance transform on the initial segmentation is introduced in place of traditional inner distance transform. The new algorithm produce smooth or straight boundaries unlike other watershed-based methods that usually produce jagged boundaries.

The experimental results show that the proposed method is more robust to noise in separating clustered nuclei than the classical watershed algorithm and condition erosion method. The proposed method generates smoother watershed lines, and thus obtains higher accuracy in nuclei separation than the earlier methods. Moreover, our experiments on several image datesets indicate that the performance is not sensitive to its parameters.

Our method is based on the presumption that there exists one-to-one correspondence between shape markers and objects. Therefore, when the size and the shape of nuclei vary a lot in one cluster, the algorithm could fail to detect the correct number of nuclei. Our algorithm mainly focuses on preventing oversegmentation while undersegmentation is not explicitly accounted for. As seen in the experiments, the proposed method generated

very few undersegmentation of cells, which is mostly due to dividing cells that are ambiguous to separate. In case of very irregular boundaries, our method may require use of more specific priors or inclusion of strong shape constraints for accurate localization of the interfaces between nuclei. When morphological hole filling was performed, our method could remove small holes that can be gaps among clustered nuclei. An algorithm based on nuclei size, the distance to nuclei centers, etc., may distinguish them from holes inside nuclei.

The future of this paper could integrate more information such as texture of intensities and *a prior* biological knowledge of the cells into the segmentation process. As the method is fully automated unlike earlier techniques [10], [11], it is suited for high throughput and spatiotemporal analysis of cell images.

ACKNOWLEDGMENT

The authors would like to thank Dr. S. Ahmad and S. Hariharan of Centre for Molecular Medicine, Singapore, for providing the microscopy images of mouse neurons.

REFERENCES

[1] M. Kass, A. Witkin, and D. Terzopoulos, "Snakes: Active contour models," *Int. J. Comput. Vis.*, vol. 1, no. 4, pp. 321–331, 1987.
[2] S. Osher and J. A. Sethian, "Fronts propagating with curvature-dependent speed: Algorithms based on Hamilton–Jacobi formulations," *J. Comput. Phys.*, vol. 79, pp. 12–49, 1988.
[3] R. G. N. Meegama and J. C. Rajapakse, "Nurbs snakes," *Image Vis. Comput.*, vol. 21, pp. 551–562, 2003.
[4] T. F. Chan and L. A. Vese, "Active contours without edges," *IEEE Trans. Image Process.*, vol. 10, no. 2, pp. 266–277, Feb. 2001.
[5] B. Zhang, C. Zimmer, and J.-C. Olivo-Marin, "Tracking fluorescent cells with coupled geometric active contours," in *Proc. IEEE Int. Symp. Biomed. Imag. (ISBI)*, 2004, pp. 476–479.
[6] A. Dufour, V. Shinin, S. Tajbakhsh, N. Guillen, J.-C. Olivo-Marin, and C. Zimmer, "Segmenting and tracking fluorescent cells in dynamic 3-D microscopy with coupled active surfaces," *IEEE Trans. Image Process.*, vol. 14, no. 9, pp. 1396–1410, Sep. 2005.
[7] A. Pinidiyaarachchi and C. Wählby, "Seeded watersheds for combined segmentation and tracking of cells," in *Proc. Int. Conf. Image Anal. Process. (ICIAP)*, 2005, vol. 3617, pp. 336–343.
[8] G. Lin, M. K. Chawla, K. Olson, J. F. Guzowski, C. A. Barnes, and B. Roysam, "Hierarchical, model-based merging of multiple fragments for improved three-dimensional segmentation of nuclei," *Cytometry Part A*, vol. 63A, pp. 20–33, 2005.
[9] P. R. Gudla, K. Nandy, J. Collins, K. J. Meaburn, T. Misteli, and S. J. Lockett, "A high-throughput system for segmenting nuclei using multiscale techniques," *Cytometry Part A*, vol. 73A, pp. 451–466, 2008.
[10] D. Baggett, M. Nakaya, M. McAuliffe, T. P. Yamaguchi, and S. Lockett, "Whole cell segmentation in solid tissue sections," *Cytometry Part A*, vol. 67A, pp. 137–143, 2005.
[11] D. P. McCullough, P. R. Gudla, B. S. Harris, J. A. Collins, K. J. Meaburn, M. Nakaya, T. P. Yamaguchi, T. Misteli, and S. Lockett, "Segmentation of whole cells and cell nuclei from 3-D optical microscope images using dynamic programming," *IEEE Trans. Med. Imag.*, vol. 27, no. 5, pp. 723–734, May 2008.
[12] Y. Boykov and G. Funka-Lea, "Graph cuts and efficient N-D image segmentation," *Int. J. Comput. Vis.*, vol. 70, no. 2, pp. 109–131, 2006.
[13] B. L. Luck, K. D. Carlson, A. C. Bovik, and R. R. Richards-Kortun, "An image model and segmentation algorithm for reflectance confocal images of in vivo cervical tissue," *IEEE Trans. Image Process.*, vol. 14, no. 9, pp. 1265–1276, Sep. 2005.
[14] G. Li, T. Liu, A. Tarokh, J. Nie, L. Guo, A. Mara, S. Holley, and S. T. Wong. (2007). 3D cell nuclei segmentation based on gradient flow tracking. *BMC Cell Biol.* [Online]. *8(40)*. Available: http://www.biomedcentral.com/1471-2121/8/40
[15] L. Vincent and P. Soille, "Watersheds in digital spaces: An efficient algorithm based on immersion simulations," *IEEE Trans. Pattern Anal. Mach. Intell.*, vol. 13, no. 6, pp. 583–598, Jun. 1991.
[16] X. Chen, X. Zhou, and S. T. C. Wong, "Automated segmentation, classification, and tracking of cancer cell nuclei in time-lapse microscopy," *IEEE Trans. Biomed. Eng.*, vol. 53, no. 4, pp. 762–766, Apr. 2006.
[17] P. S. U. Adiga and B. B. Chaudhuri, "An efficient method based on watershed and rule-based merging for segmentation of 3-D histo-pathological images," *Pattern Recognit.*, vol. 34, pp. 1449–1458, 2001.
[18] F. Meyer and S. Beucher, "Morphological segmentation," *J. Vis. Commun. Image Representation*, vol. 1, no. 1, pp. 21–46, 1990.
[19] N. Malpica, C. O. de Solrzano, J. J. Vaquero, A. Santos, I. Vallcorba, and J. M. Garcła-Sagredo, F. del Pozo, "Applying watershed algorithms to the segmentation of clustered nuclei," *Cytometry*, vol. 28, pp. 289–297, 1997.
[20] X. Yang, H. Li, and X. Zhou, "Nuclei segmentation using marker-controlled watershed, tracking using mean-shift, and Kalman filter in time-lapse microscopy," *IEEE Trans. Circuits Syst. I, Reg. Papers*, vol. 53, no. 11, pp. 2405–2414, Nov. 2006.
[21] K. Z. Mao, P. Zhao, and P.-H. Tan, "Supervised learning-based cell image segmentation for p53 immunohistochemistry," *IEEE Trans. Biomed. Eng.*, vol. 53, no. 6, pp. 1153–1163, Jun. 2006.
[22] P. Soille, *Morphological Image Analysis: Principles and Applications*. New York: Springer-Verlag, 1999.
[23] S. Beucher and F. Meyer, "The morphological approach to segmentation: The watershed transformation," in *Proc. Math. Morphol. Image Process.*, 1993, pp. 433–481.
[24] R. Beare and G. Lehmann. (2006, Jan.–Jun.). The watershed transform in ITK—Discussion and new developments. *Insight J.* [Online]. Available: http://www.insight-journal.org/browse/journal/4
[25] F. Meyer, "Topographic distance and watershed lines," *Signal Process.*, vol. 38, no. 1, pp. 113–125, 1994.
[26] T. R. Jones, A. E. Carpenter, and P. Golland, "Voronoi-based segmentation of cells on image manifolds," in *Proc. ICCV Workshop Comput. Vis. Biomed. Image Appl. (CVBIA)* (Lecture Notes in Computer Science), Y. Liu, T. Jiang, and C. Zhang, Eds., 2005, vol. 3765, pp. 535–543.

Jierong Cheng received the B.E. degree in electrical engineering from Zhejiang University, Hangzhou, China, in 2002, and the Ph.D. degree in electrical and electronic engineering from Nanyang Technological University, Singapore, in 2007.

She is currently a Postdoctoral Research Fellow at the BioInformatics Research Centre, Nanyang Technological University. She is also with the Computation and Systems Biology Programme, Singapore–Massachusetts Institute of Technology (MIT) Alliance, Singapore. Her current research interests include biomedical image analysis, active contours, and image segmentation.

Jagath C. Rajapakse (S'90–M'91–SM'00) received the M.Sc. and Ph.D. degrees in electrical and computer engineering from the University at Buffalo, Buffalo, NY.

He is currently a Professor of computer engineering and the Director of the BioInformatics Research Centre, Nanyang Technological University (NTU), Singapore. He is also Visiting Professor in the Department of Biological Engineering, Massachusetts Institute of Technology (MIT), Cambridge. He was a Postdoctoral Researcher at the Max-Planck Institute of Cognitive and Brain Sciences, Germany, and the National Institute of Mental Health, USA. His current research interests include neuroinformatics and bioinformatics. He has authored or coauthored over 210 research papers in refereed journals, books, and conference proceedings. He was listed among the most cited scientists of all fields.

Prof. Rajapakse is an Associate Editor of the IEEE TRANSACTIONS ON MEDICAL IMAGING, the IEEE TRANSACTIONS ON COMPUTATIONAL BIOLOGY AND BIOINFORMATICS, and the IEEE TRANSACTIONS ON NEURAL NETWORKS.